High Order Methods for Helmholtz Problems in Highly Heterogeneous Media

Hélène Barucq, Henri Calandra, Théophile Chaumont-Frelet, Christian Gout

High Order Methods for Helmholtz Problems in Highly Heterogeneous Media

H. Barucq[a], H. Calandra[b], T. Chaumont-Frelet[a,c], C. Gout[c]
[a]INRIA EPI MAGIQUE3D, [b]TOTAL EP, [c]LMI INSA-ROUEN

Introduction

We consider the acoustic Helmholtz equation with constant density

$$\begin{cases} -\dfrac{\omega^2}{c^2}u - \Delta u = f & \text{in } \Omega, \\ \nabla u \cdot \mathbf{n} - \dfrac{\mathbf{i}\omega}{c}u = 0 & \text{on } \Gamma_A, \\ u = 0 & \text{on } \Gamma_D, \end{cases} \tag{1}$$

where u is the pressure, ω is the angular frequency, f is the source of excitation and c is the heterogeneous velocity parameter.
When discretizing problem (1) with a finite element method, the mesh induces an approximation of the velocity parameter c if it does not fit the interfaces. This is troublesome for high order methods, where a coarse mesh is usually used, with several degrees of freedom per cell.
We improve the performance of high order methods in highly heterogeneous media, by refining the approximation of the velocity parameter without changing the finite element mesh (see figure 1 and 2).

Basic FEM

The basic finite element technique to assemble the associated linear system consists in assuming that the velocity is constant on each cell K. That way, one can store the reference values

$$\hat{M}_{ij} = \int_{\hat{K}} \hat{\phi}_j \hat{\phi}_i,$$

where $\hat{K}$ is the reference cell and $\hat{\phi}_j, \hat{\phi}_i$ are the shape functions, and use the linear mapping onto the actual cell K to compute the entries

$$\int_K \frac{1}{c^2}\phi_j\phi_i = \text{area } (K)\frac{1}{c_K^2}\hat{M}_{ij}.$$

Medium approximation

We improve the basic methodology by subdividing the reference cell into a submesh $\{\hat{A}_l\}_{l=1}^{n_s}$, and storing the reference values

$$\hat{M}^l_{ij} = \int_{\hat{A}_l} \hat{\phi}_j \hat{\phi}_i.$$

for $l \in \{1, \dots, n_s\}$. Therefore, we only need to assume that c is constant on the images of the subcells (yielding a finer approximation of the medium) and compute the entries with

$$\int_K \frac{1}{c^2}\phi_j\phi_i = \text{area } (K)\sum_{l=1}^{n_s}\frac{1}{c_{K,l}^2}\hat{M}^l_{ij}.$$

That way, we keep the usual stencil of the linear system of the basic FEM, but each coefficient is weighted differently because the approximation of c is improved.
It follows that the inversion of the linear system has the same cost. Only the time for matrix assembling is multiplied by n_s, but this preprocessing step can be easily parallelised.
Figure 1 and 2 illustrate the improvement that our methodology can bring on coarse meshes.

Marmousi test-case

We present our methodology on the Marmousi test-case at the fequency $f = 10$Hz and a Dirac source term at $(2000, 100)$. We use a coarse mesh of 2342 triangles and $\mathcal{P}_6$ elements. Figure 1 shows how well the velocity model is handled by the mesh without subdision ($n_s = 1$) and with $n_s = 64$ subdivisions of the reference cell.

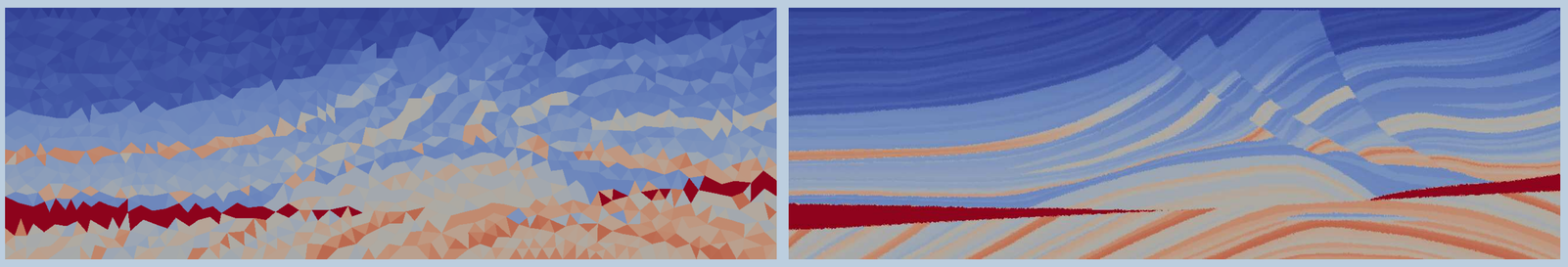

Figure 1: Basic medium approximation (left); 64 subcells (right)

Figure 2 shows a zoom. We see that the finite element mesh is preserved, but each cell is subdivided into $n_s = 64$ subcells.

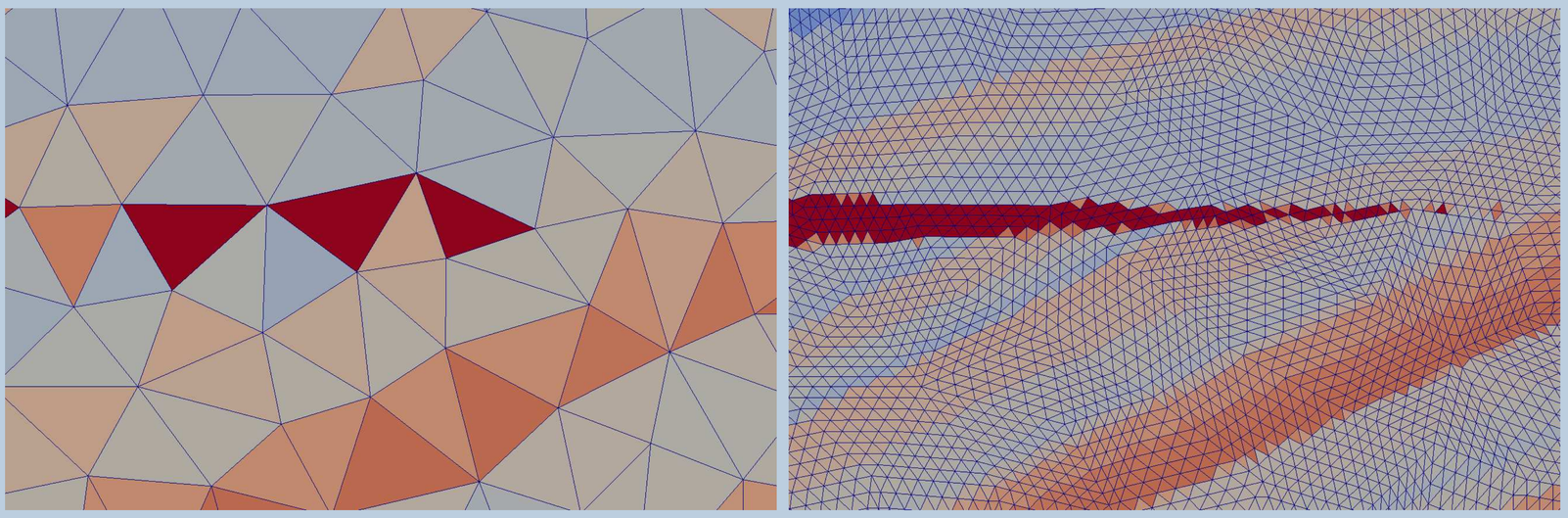

Figure 2: Basic medium approximation (left); 64 subcells (right)

In order to compare the two methodologies, we compute a reference solution with $\mathcal{P}_6$ elements on a much finer mesh of 95488 triangles. Figure 3 presents a cut of the three differents solutions. We see that the numerical solution computed with $n_s = 64$ subcells is much closer to the reference solution. Yet, the computational cost for this solution is roughly the same as the basic FEM. As a conclusion, Table 1 confirms that the quality of the solution is increased when the velocity approximation is refined.

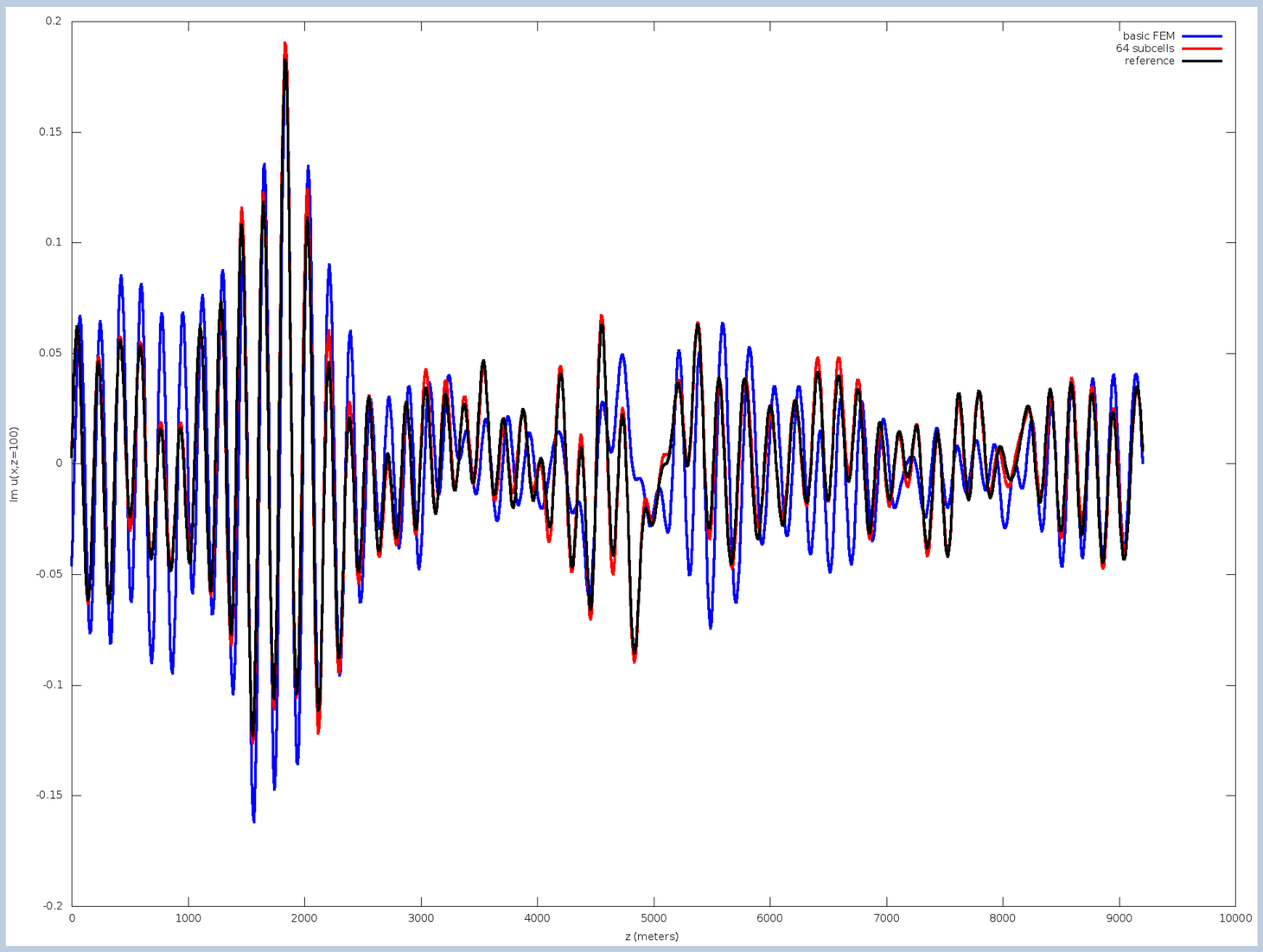

Figure 3: Cut of the numerical solutions at 100m depth (imaginary part)

n_s	relative L^2 error	n_s	relative L^2 error
1	70.9%	64	11.2%
4	36.7%	256	8.24%
16	14.5%	1024	7.91%

Table 1: Relative error on the cut